

Flame Length and Geometry as Key Indicators for Real-Time Thermal Stress Monitoring in a Multi-Burner Combustion Chamber

Matthias Arnold¹, Mareike Hoyer¹, Sina Keller^{1,2}

¹ ci-tec GmbH, 76139 Karlsruhe, Germany - (m.arnold, m.hoyer)@ci-tec.de

² Institute of Photogrammetry and Remote Sensing, Karlsruhe Institute of Technology, 76131 Karlsruhe, Germany - sina.keller@kit.edu

Keywords: Industrial Burner Flames, Combustion Control, 2D Measurements, Flame Length, Deep Learning.

Abstract

This study investigates the relationship between flame length measurements and the temperature of the refractory lining in combustion chambers with multiple burners interacting in terms of fluid dynamics. As this has not been done before, this study investigates the general feasibility and can serve as a baseline for future studies. The data stems from the post-combustion chamber of a hazardous waste incineration plant, where waste is burned at very high temperatures to minimize pollution. It was recorded by a near-infrared camera, which samples pixel-wise temperatures with a frequency of 50 Hz. Four burners mounted at the same height are considered within the chamber, producing four flames mutually influencing each other. The flames are segmented with a deep-learning model. The acquired flame masks serve as a basis to determine individual flame properties. We introduce burner axis flame length and medial axis flame length and show that the shape or bending of a flame can be deduced depending on the relationship between those two lengths. Combined with their magnitude, these lengths indicate whether certain parts of the refractory wall are at risk of exposure to thermal stress, making the implementation of an automatic, generalizable, and transparent combustion control system feasible. Finally, we also highlight that all burners must be considered for effective automatic control in a complex multi-burner geometry. This system optimizes burner settings based on the observed and measured flame geometry, maximizing throughput while minimizing refractory wear, thus improving sustainability.

1. Introduction

Over half of the world's CO₂ emissions stem from the energy and industrial sectors. Industrial high-temperature and combustion processes are responsible for the largest share of these emissions, according to the European Commission (2020). The growing concern over climate change and its direct link to CO₂ emissions has emphasized the urgent need for sustainable solutions and stimulated intensive research towards decarbonizing the process industry. Although the measures to reduce the environmental impact are already having an effect and will continue unabated, there are limits since some of the emissions are inherent to the respective process and cannot be entirely prevented (as in the calcination process of cement production or waste incineration). Although carbon capture, utilization, and storage technologies have become essential for achieving net zero, they can only serve as a last resort. Consequently, further optimization and advanced process control strategies have become crucial for reducing emissions and enhancing sustainability.

The optimization of industrial combustion processes is based on several pillars, including offline approaches focused on optimizing the ideal steady state and online optimization. Research efforts range from improving the processes themselves to optimizing entire plants. Experimental insights and findings from plant operation during maintenance downtimes are complemented by numerical methods like computational fluid dynamics, a powerful tool for understanding and designing, e. g., more efficient burners and combustion chambers like Yang et al. (2002). Effective online optimization builds on detailed and reliable information about the current process state, delivered by adequate sensor equipment installed throughout the plant and in the combustion chamber. Ideally, a fully automated control system can be set up to adapt to dynamic changes and ensure optimal plant

operation. This is as important as it is challenging in those applications involving fuels of fluctuating composition or with otherwise highly variable properties such as their moisture and calorific value. These fuels, e. g., refuse-derived fuels employed as alternative fuels to decarbonize cement production or utilized for energy generation, necessitate constant adaptation of burner settings. In reality, owing to the complex dynamics, only parts of the process are entirely automatized, and optimal set points for operation often have to be determined by experienced operators in the control room, leaving the control partly open-loop. To set up an effective closed-loop control for the combustion process, including automatic burner control, three requirements have to be met: (i) the availability of detailed information, (ii) continuous in an automated and quantitative manner, and (iii) options to adjust the relevant settings accordingly. This paper contributes to closing the gap by addressing the second aspect: We introduce a generalizable approach to flame-feature extraction that is particularly suited for complex multi-burner setups and demonstrate the application potential of the proposed novel flame properties.

As an application example, we consider post-combustion chambers of rotary-kiln-based hazardous waste incineration plants (see Figure 1 for an overview), which are ideally suited for deriving generalizable solutions due to their multi-burner geometry with the inherent need to consider the challenges associated with complex dynamics of interacting flames. Furthermore, the complex interplay of various ecological, safety, and economic objectives in hazardous waste incineration, such as maintaining minimum temperatures, ensuring complete burnout, maximizing energy recovery, and optimizing throughput while reducing emissions, stabilizing the process, and minimizing refractory wear, highlights the importance of a sophisticated control system. State-of-the-art facilities employ comprehensive

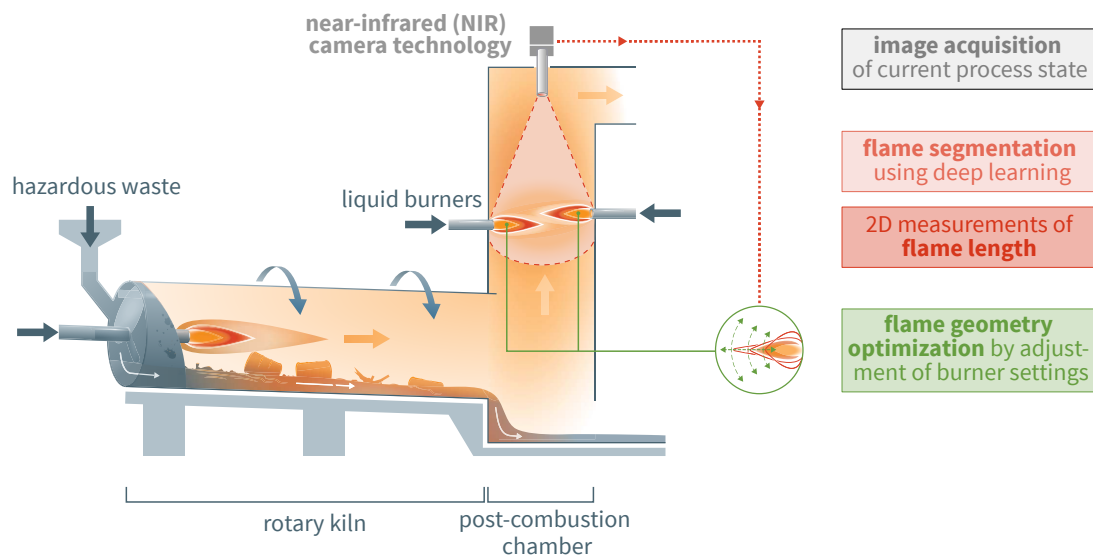


Figure 1. Schematic of the combustion section of a hazardous waste incineration plant, with a rotary kiln and a post-combustion chamber. In the post-combustion chamber, various burners are mounted to the walls. Their flames can be visualized using an NIR camera installed at the chamber's ceiling. The encoded information can be used to optimize the flame shape by adjusting the burner settings. The corresponding image-processing flow for automatic parameter extraction proposed in this paper is shown at the right.

process and plant technology to ensure safe and efficient operation. Regulatory compliance is maintained through stringent monitoring of temperatures and emissions, with automatic shut-downs in place for violations. However, the primary focus is often on global parameters, such as temperature and emissions. In contrast, local phenomena, such as the spatial distribution of temperatures and flame characteristics (like flame length) within the combustion chamber, can provide valuable insights for optimization. Infrared (IR) camera technology offers an excellent way to capture this spatial information, yet translating it into actionable control inputs, especially closed-loop, remains challenging. It is a precious tool that regularly provides operators with real-time visual feedback on combustion conditions, thereby allowing for improved manual optimization of burner settings. In principle, state-of-the-art image processing (including artificial intelligence (AI) methods) can automatically extract quantitative information characterizing the current process state from IR images recorded in the combustion chamber. However, identifying meaningful metrics for utilization in combustion control is not straightforward since parameters must be identified in the images, which can be linked to a controllable root cause. Parameters such as flame length, structure, and wall temperatures are interesting, although they vary significantly with operational conditions. Furthermore, it depends on plant specifics, such as the number of burners and their arrangement, which of the available parameters would be suitable process values for automatic control. One further aspect of successfully implementing technological innovations into a plant's control scheme is the transparency and explainability to human operators. This poses additional challenges for leveraging AI's novel possibilities, particularly deep-learning (DL) methods, to extract characteristic parameters automatically.

To tackle that, this paper presents an approach to subsequent flame segmentation and feature extraction, combining DL image processing methods for pixel-wise flame detection with process knowledge for performing 2D flame measurements. This two-stage approach enhances transparency and reduces the risk of model performance degradation over time since AI is only used to solve the rather generic task of flame segmentation.

Last but not least, it facilitates the approach's generalizability to other plants and similar applications. For example, this could prove highly useful in the transformation towards green hydrogen with its differing combustion behavior. As a result, this paper presents novel parameters for real-time monitoring and closed-loop control of multi-burner combustion systems and a robust method for automatically and in real-time obtaining this information in the post-combustion chamber of a hazardous waste incineration plant. The proposed approach optimizes burner settings dynamically by leveraging advanced sensor technologies and data-driven models, ensuring safe, efficient, and sustainable operation. Specifically, metrics for measuring the length of a flame based on near-infrared (NIR) imaging technology are considered since they are of interest from a maintenance perspective: While the throughput should be high to use the plant's optimal capacity, a high thermal load damages the refractory lining and should be kept to the minimum required for complete burnout. Flames with a potentially damaging extent to the refractory lining should hence be detected early to optimize the corresponding burner settings (swirl, axial air, fuel mass flow rate) as far as possible. Therefore, we assess the proposed characteristic parameters' potential to capture undesirable process states in multi-burner systems by analyzing their thermal effect on the combustion chamber wall. As a word of caution, the analysis is based on real-world data from a plant in which the processes are already optimized manually. Hence, the statistical significance of those results can only be limited. Still, they strongly indicate that the proposed parameters can be of practical use. Moreover, our results provide an essential baseline for similar future research.

2. Related Work

The use of *advanced process control systems*, often even combined with the installation of IR cameras, for online optimization of the combustion process is a well-established standard in plants of the process industry around the world. They are ranked among the best-available techniques for waste incineration by the European Commission (2019) and ensure safe 24/7

operation. However, due to the manifold challenges presented in Section 1 associated with further (online and offline) optimization of industrial combustion processes and additionally driven by the associated high ecological as well as economic rewards, this remains a highly active field of research and product development. Since classical PID controllers are insufficient for complex multivariable systems, various approaches have been introduced, including fuzzy logic, model-predictive control, and digital twins (Tang et al. (2024), Hammerschmid et al. (2023)). Yet even more critical for successful automatic, proper closed-loop control in process plants is detailed real-time information about the current process state, which is a prerequisite for dealing with fast dynamics, particularly in industrial combustion processes. Advances in sensor equipment and increased computation power have enabled new possibilities to collect, analyze, and utilize data throughout process plants in an automated fashion. In particular, AI methods offer new options for solving complex problems in a data-driven manner, as summarized by Shang and You (2019) in the context of the process industry. While AI is already routinely applied in many applications, from autonomous driving and industrial automation to medical imaging, its implementation in the process industry is still in its infancy, and most studies are purely academic. Of the many exciting ideas and promising research results related to this work, we highlight work on soft sensors for the process industry and flame characterization in industrial combustion processes.

Soft sensors are a beneficial complement for hardware sensors whenever they are unavailable, for technological reasons, high costs, or because sensor installation in the plant is complicated or hindered due to challenging conditions. Soft sensors combine the input of existing sensor equipment to calculate novel process characteristics in real time. This can be achieved by models based on detailed expert knowledge about the processes or by using AI in a data-driven manner. The latter corresponds to a supervised regression task and has gained popularity for model development. Kadlec et al. (2009) and Jiang et al. (2021) summarize areas of promising application together with the inherent, in parts severe, challenges characteristic for the process industry: heterogeneity and quality of the data, drifts of sensors and processes, and co-linearity, which require thorough data preparation and curation along with regular maintenance. Recent soft-sensor developments which constitute a valuable input for improving process control of industrial combustion processes are related to the estimation of emissions (Klier (2023), Bunsan et al. (2013), Norhayati and Rashid (2018), Xia et al. (2024)) and (e. g., for co-incineration in cement plants) product quality (Ali et al. (2022), Pani et al. (2013)).

Different sensor technologies are available for directly assessing flame properties and their continuous monitoring in practical applications, as summarized by Ballester and García-Armingol (2010). The most direct feedback on the current combustion process can be accessed by camera technology installed inside the combustion chamber. Depending on the composition of the combustion atmosphere and the details of interest (refractory lining of the combustion chamber, the fuels, or the flame bodies), appropriate camera technology with a suitable spectral range can be selected for visualization. Using image processing to automatically interpret the corresponding (IR) images and extract relevant features has sparked research interest but is not routinely used for process control. *Flame parameters* with application potential for automatic flame assessment in industrial combustion processes consider geometrical, lumin-

ous, and color characteristics, primarily based on conventional image-processing methods. Those can be used to make quantitative comparisons of novel burner set-ups (Lee et al. (2021)) and different modes of operation (Yan et al. (2002)). Using three CCD cameras, even a three-dimensional flame model has been proposed for detailed monitoring by Lu et al. (2005). The idea of using vision systems for furnace control and waste-to-energy plants is also present in the literature, e. g., presented by Lu et al. (1999) and Zipser et al. (2006). This is especially relevant for the dynamic adaptation of burner settings in the context of varying fuel properties of refuse-derived alternative fuels and waste incinerators. Matthes et al. (2023) proposed a novel measure of flame stability in image sequences. *Flame length* has also been considered in the literature. However, the existing definitions are limited to the single-flame case, as flame length is usually defined with respect to a straight horizontal (or vertical, depending on the orientation of the burner) „centerline“ of the flame starting at the burner tip. Regarding the endpoint, different definitions (associated with various methods to measure them) can be found in the literature, as summarized by, e. g., Becker and Liang (1978) or Chu et al. (2024). The most common definition is based on the position where the stoichiometric condition occurs, which is particularly useful from the viewpoint of chemistry to compare flames as manifestations of exothermic reactions. However, it is not practical for industrial applications. Other definitions are based on (thermographic) imaging techniques, defining the endpoint based on the temperature distribution along the centerline or straightforwardly using the flame tip of the visible part of the flame with regard to the centerline. A generalization appropriate to quantify the properties of the highly interacting flames in multi-burner geometries of industrial combustion chambers—where the concept of the centerline is not straightforward—has not been established yet. Utilization in practical applications requires that the derived parameters encode meaningful information about the process state. As a data-driven alternative to expert knowledge, the relation of novel parameters to other measurements can be analyzed to assess their usefulness. For example, as a performance test, Hernández and Ballester (2008) used the capability to estimate NO_x emissions (closely linked to the combustion conditions).

While the extensive research efforts and, e. g., the position paper of the ProcessNet Expert Group "Waste Treatment and Recycling" (2022) underline the interest in viable solutions, there is still a shortfall of already existing geometric measurements concerning their applicability in multi-burner settings with strongly interacting flames. The recent availability of DL models for flame segmentation (Großkopf et al. (2021), Landgraf et al. (2023a)) offers the possibility to segment multiple and even partly overlapping flames. Thus, the image-based flame characterization by characteristic parameters also becomes feasible in more complex plant geometries for the first time. Klier (2023) already considered flame lengths in a multi-burner setting using parts of the same data; we built on their definitions and refined them for our purpose. In addition, by investigating the relationship between flame lengths and combustion chamber wall temperatures, we establish for the first time the potential of novel flame length definitions for practical applications.

3. Data

The NIR image data, on which this study is based, was recorded for almost 1.5 years in the post-combustion chamber of a state-of-the-art industrial hazardous waste incineration plant.

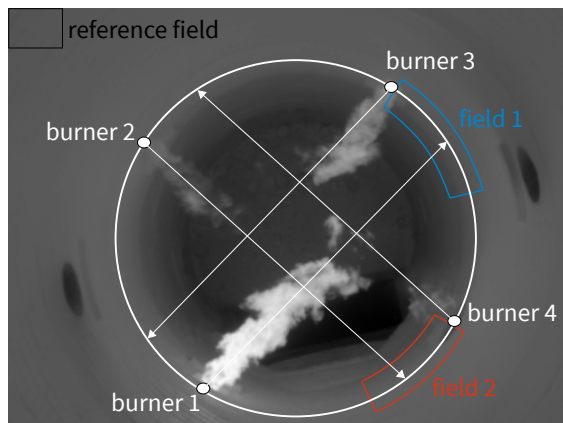


Figure 2. Thermal image of the chamber with all burners active. The burner starting points, as well as their axes, are included. The circle accentuates the geometry of the chamber on the burner level. Finally, three temperature fields are highlighted.

The camera technology and measurement setup are described in Section 3.1. More details on the dataset are presented in Section 3.2. Since the data is firmly protected within the industry, the dataset cannot be made available. A comparable dataset, however, in the visual spectral range, was published by Landgraf et al. (2023b).

3.1 Measurement Setup

A typical hazardous waste incineration plant design is shown schematically in Figure 1. It combines a (slightly tilted) rotary kiln and a post-combustion chamber to ensure the safe and environmentally friendly disposal of various hazardous materials in solid, pasty, liquid, and gaseous form in compliance with the regulatory requirements. The top view of the circular post-combustion chamber shows the walls with several burner openings and the opening of the rotary kiln. The liquid burners analyzed here are installed at equal angular intervals and the same height as the post-combustion chamber.

The image data (see Figure 2 for an example) has been recorded at a frequency of 50 Hz using the PYROINC 768N model by DIAS, with a spectral range of $0.8\ \mu\text{m}$ to $1.1\ \mu\text{m}$ (near infrared). This spectral range is characterized by low transmission through the flames' soot; hence, this technology is applicable to visualize the flame bodies (Waibel, 2014). Exceptions are pure fuels such as natural gas or fuels with a high water content, which burn with flames that are mostly transparent in the NIR range. The sensor has $768\ \text{pixel} \times 576\ \text{pixel}$, and the resulting images contain pixel-wise temperature information in the temperature range $600\ ^\circ\text{C}$ to $1500\ ^\circ\text{C}$, subject to measurement uncertainty of 2% (3% for object temperatures above $1400\ ^\circ\text{C}$). If necessary, it is calibrated every one and a half years using a black body. The camera was inserted into the post-combustion chamber through a guiding tube at its top, and it was equipped with protective measures (cooling and cleansing) appropriate for 24/7 operation.

3.2 Dataset

For our analysis, we rely on 879 frames showing different situations in the post-combustion chamber. The selection was drawn from frequent measurement campaigns conducted over almost 1.5 years with the setup described in Section 3.1. The dataset

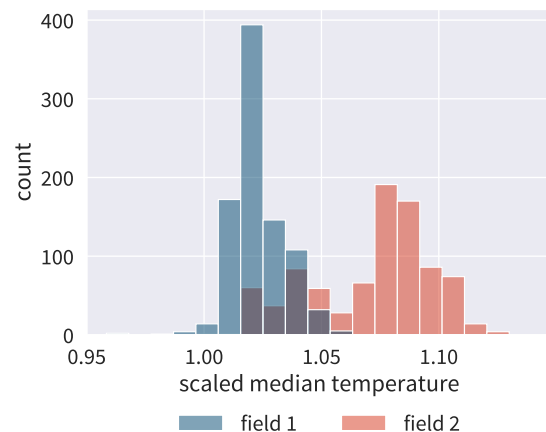


Figure 3. Scaled temperature distribution for all frames distinguished by field.

covers the range of typical process situations relevant to automatic control, with all prevalent combinations of active burners present. One exemplary situation is shown in Figure 2 as a grayscale image, where the temperature range of this image was mapped to 0 to 255. Each frame contains up to four burner flames, and individual burners can be turned on and off individually for process control. Additional flames could emerge from the two natural gas burners (visible as dark holes on the left and right of Figure 2) and the rotary kiln at the bottom. However, these flames have been excluded from our analysis. The undisturbed fuel trajectory of each burner is indicated by an arrow in Figure 2.

From the three regions denoted as *field 1*, *field 2*, and *reference field*, we extract spatially averaged temperatures using the median to be robust concerning outliers. Field pixels that are covered by flames are excluded from the median. We chose the specific positions of field 1 and field 2 because they are good examples of different thermal stress situations. The reference median temperature of the reference field is used to scale the extracted temperatures of field 1 and field 2. The scaling is done since the overall temperature in the chamber can vary considerably, and we regard the upper left corner (showing only the wall of the post-combustion chamber, not influenced by any burner) as sufficiently robust to short-time fluctuations throughout all recorded data. Figure 3 shows the scaled temperature distributions for both fields over all frames. Within our dataset, both fields are hotter than the reference field, with field 2 often reaching higher temperatures than field 1.

4. Methodology

This section will present our procedure as outlined in Figure 1. First, we describe the details of the segmentation process. Afterward, we introduce the flame lengths investigated in this work.

4.1 Flame Segmentation

We rely on an updated version of the DL model introduced by Landgraf et al. (2023a) to segment flames. It generates one flame mask per burner. The segmentation results are then post-processed using scikit-image (van der Walt et al., 2014) in two steps: Firstly, holes in the flames are removed, and secondly, the number of segmented flame areas per burner is limited to

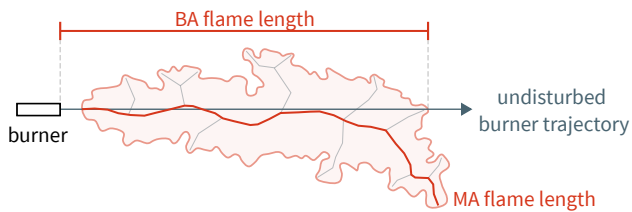


Figure 4. Schema of both flame lengths. The BA flame length is the distance between the burner position and the last pixel of the segmented flame along the undisturbed burner axis. The MA flame length is the longest path of the flame skeleton extracted from the largest segmented flame area.

one. Since not all flames have one body, the DL model might (correctly) detect several disconnected regions. Smaller regions are dropped, and flame lengths are extracted from the most significant connected component. An example result of the final segmentation can be seen in Figure 5.

4.2 Flame Length

We focus on two flame lengths in this study: *burner axis (BA) flame length* and *medial axis (MA) flame length*, which are illustrated in Figure 4 as well as Figure 5. All lengths have been scaled concerning the chamber cross section at burner level using the respective burner axes, i. e., the arrows' lengths depicted in Figure 2 are the corresponding scaling factors.

4.2.1 BA Flame Length The BA flame length describes the distance between the burner location and the most distant segmented pixel along its (undisturbed) fuel trajectory, i. e., along the burner axis. This property generalizes (to arbitrarily positioned burners) what is usually referred to as flame length in the literature, which is especially beneficial in the context of a single burner with an undisturbed flame. A BA flame length example for burner 1 can be seen on the left side of Figure 5. A line is included, showing the burner's fuel trajectory over the entire chamber cross-section. The line color is red for parts overlapping with burner 1's flame; otherwise, it is white. The red segment represents the BA flame length, which, when scaled to the full chamber length, scores a value of 0.49 in this example. Generally, the BA flame length lies between 0 and 1 but can also become slightly larger than 1 (cf. Figures 6 and 7) if the flame reaches the opposite wall and is deflected upwards.

4.2.2 MA Flame Length We extract the skeleton of a segmented flame mask using the Zhang method (Zhang and Suen, 1984) as implemented in scikit-image (van der Walt et al., 2014). We rely on the „analyze_skeletons“ method of the Python package „FilFinder“ (Koch and Rosolowsky, 2015) for further analysis. It can extract the longest path within a skeleton as illustrated in Figure 5. We refer to the length of the longest path as MA flame length. As mentioned, we remove holes in the segmented mask before the skeleton extraction as they can cause a deceptively long MA flame length. We highly weigh the skeleton pixel closest to the burner to ensure that the longest path's starting point is always near the burner. Weighting can be achieved by giving this pixel a higher value in an otherwise binary mask. Again, the MA flame length is scaled by the full chamber length, resulting in 0.75 in Figure 5. As the MA flame length is not straight, it can be longer than the full chamber length, leading to values that are considerably greater than one. The extensive range of obtained MA flame lengths (see Figures 6 and 7) reflects the variety of flame shapes in the dataset.

5. Results and Discussion

To demonstrate the application potential of the flame lengths defined in Section 4.2 for flame control, particularly for the multi-burner scenario, we evaluate their information content about the damage potential of flames touching the refractory lining. High temperatures are related to thermal stress. However, this information needs to be traced to its source to adapt the burner settings accordingly.

We focus on burner 1 and burner 2 in this analysis, as they have the highest variation in length. We defined fields 1 and 2 so that they are positioned where the respective burners' undisturbed fuel trajectory would hit the opposite wall. Furthermore, field 2 covers the wall where the flame of burner 1 hits the wall when it's strongly affected by burner 2. This problem is, of course, symmetric and could be generalized to all other burners. However, here, we concentrate on those examples where the benefit of the novel parameters and their interplay can be most clearly analyzed and discussed.

Regarding field 1, Figure 6 shows both the MA flame length and the BA flame length of each frame, color-coded by the scaled median temperature of the field 1. As expected, field 1 has a comparatively low median temperature when the BA flame length is small. Moreover, a high MA flame length and a BA flame length below 0.8 do not necessarily lead to high temperatures. In this area, the flame usually bends towards its right (due to the effect of burner 2) and thus does not reach the opposite wall. Accordingly, the field 1 has no high temperatures. One cluster, however, is distinguishable: When the BA and MA flame lengths are high and almost equally significant, the field 1 is approximately 5% warmer than the reference field. This cluster represents frames during which burner 1's flame is straight and long and thus reaches the opposite wall. An example where the flame is straight, and both lengths are comparably long, can be seen in Figure 2. However, the flame is too short to reach the wall. Hence, the relation between BA flame length and MA flame length can be used to identify flames with a high potential for thermal stress at the opposite wall of the combustion chamber. Burner settings can thus be adjusted before the refractory heats up, reducing permanent damage as a benefit. This intuitive finding is easily generalizable to other geometries. However, due to the complex interplay of the flames in a multi-burner geometry, flames cannot be considered isolated.

To show a more elaborate analysis, we rely on field 2. The data is shown in Figure 7, where we highlighted two counter-intuitive clusters. These clusters show that all flames must be monitored due to their interaction in a multi-burner system. The cluster on the bottom left would have a naive expectation that the wall temperature in the field 2 is low since the burner 1 flame is short. This is, however, not the case; this cluster reaches scaled temperatures of around 1.08. Another cluster (where both lengths are considerable) reaches high temperatures. Following our previous argumentation, this would indicate a very straight flame. In both cases, the field 2 should not be reached by the flame of the burner 1. Burner 2 is responsible for this, as it has a vast and straight flame in these frames, which hits the field 2 and causes high temperatures. Analogous to field 1 and burner 1, field 2 is opposite burner 2. Thus, such a setting can be avoided by additionally monitoring the burner 2's BA flame length and MA flame length.

We filtered out cases with a BA flame length of burner 2 higher

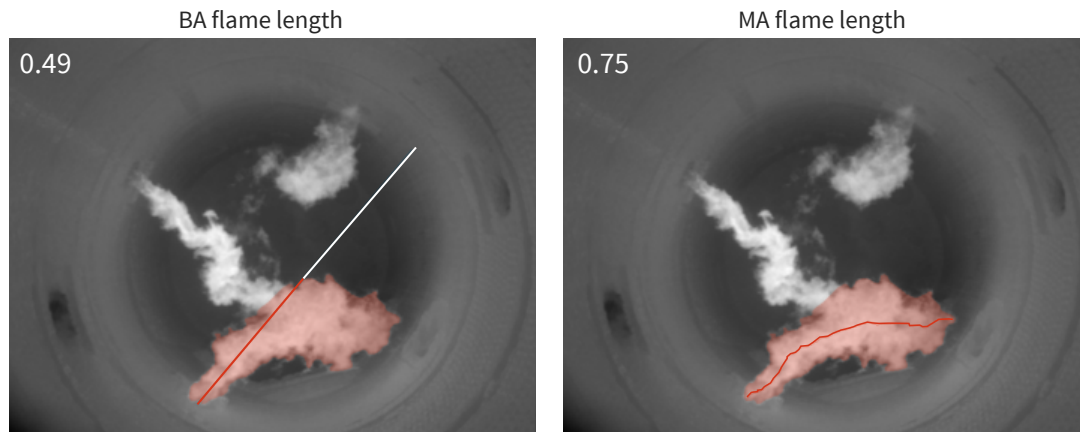


Figure 5. Examples for BA flame length and MA flame length for burner 1. The red shading also shows the segmentation results of the DL model after post-processing. The undisturbed fuel trajectory of the burner 1 is illustrated by the white line in the left image, and its overlap with the segmented flame (red) is colored in red. The length of the red part is the BA flame length. The red curvy line in the red flame represents the longest skeleton path; its length is the MA flame length. Both scaled lengths for this example images are denoted in the top-left corner of the images.

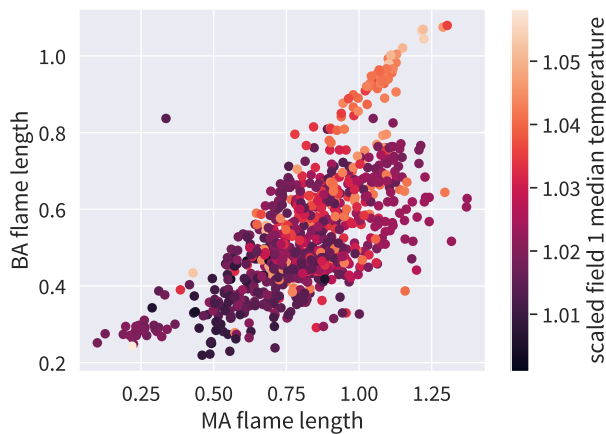


Figure 6. Scatter plot of BA flame length versus MA flame length of burner 1. Each dot represents one frame and is colored according to the scaled median temperature of the field 1.

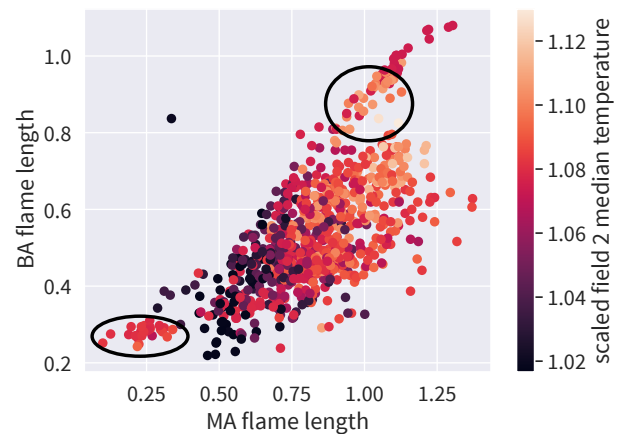


Figure 7. Scatter plot of BA flame length versus MA flame length of burner 1. Each dot represents one frame and is colored according to the scaled median temperature of field 2. Two clusters are highlighted.

than 70% of the chamber cross-section for a deeper analysis. The results can be seen in Figure 8. In the remaining cases, a small flame correlates with a minor temperature difference between the field 1 and the reference field. It also shows that an increased MA flame length leads to higher temperatures. The median of field 2 can become over 10% hotter than the reference field median. This is also the case for smaller BA flame lengths. An example of this can be seen in Figure 2. The flame is bent towards its right, reaching the field 2. High temperature occurs mainly when the MA flame length is between 0.75 and 1.2, and the BA flame length is between 0.5 and 0.8. Thus, the ratio of two lengths can be used to conclude the shape of the flame. This knowledge can then indicate the extent of the thermal stress on adjacent fields, such as field 2. Again, this is a relatively intuitive fact. However, it demonstrates the novel MA flame length's potential to contain crucial information about the flame shape in an explainable and utilizable way. Since these flame measurements can be extracted in real-time with high transparency, they can easily be included in a closed-loop process control system for optimized burner settings. This finding could also be generalized to other geometries: an MA flame

length disproportionate to the BA flame indicates a strongly bent flame. Then again, the described situation does not always cause high relative temperature differences as illustrated in Figure 8. This can partially be attributed to several limitations of this study: first, for the wall to be heated more than usual, it has to be exposed to flames for a longer period. Brief flame outbursts could reach a field but not heat it measurably, and these situations could lie within our dataset, as we sampled randomly. Smoothing the calculated parameters over time could be helpful when integrating the flame lengths into an automatic control system. Secondly, a long MA flame length does not necessarily mean the flame is bent towards the wall, as depicted in Figure 9. Since the MA flame length measurement is not performed in a specific direction, the skeleton of a profoundly branching flame can be difficult to anticipate and interpret. Especially, as in Figure 9 the MA flame length tail does not bend towards the wall, yet a large amount of the flame body affects it. Similar situations arise in approximately 5% of the evaluated images. Finally, the pixel-wise measurement uncertainty of the camera lies within the range of our scaled median temperature

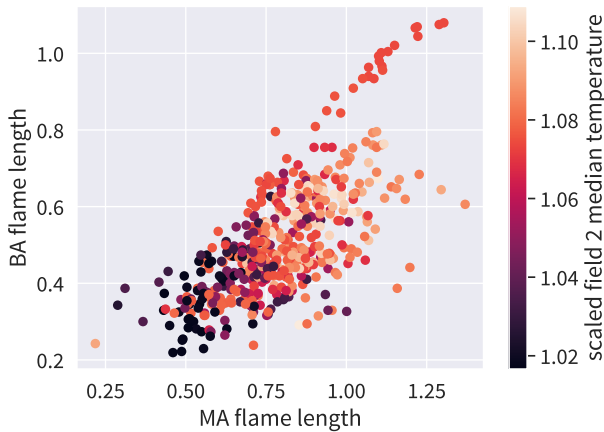


Figure 8. Scatter plot of BA flame length versus MA flame length of burner 1. Each dot represents one frame and is colored according to the scaled median temperature of field 2. Samples with a burner 2 BA flame length > 0.7 have been removed.

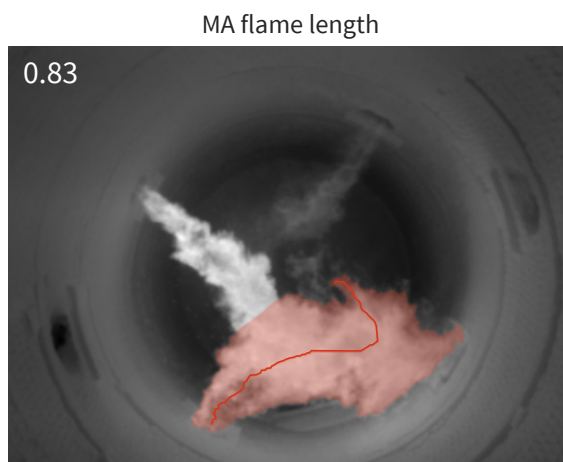


Figure 9. Example of how MA flame lengths might bend away from the wall rather than following the perceived main body.

difference. Single samples might, therefore, not be meaningful. However, as we rely on clusters and trends for our deductions, we still believe they are accurate.

6. Conclusion

This study introduces two methods for measuring flame length in near-infrared (NIR) imagery: burner axis (BA) flame length and medial axis (MA) flame length. The BA flame length measures the flame along the burner's trajectory, while the MA flame length identifies the longest skeleton path within a generated flame mask. We utilize a deep learning (DL) model for pixel-wise flame segmentation and analyze data from an industrial hazardous waste incineration plant with multiple interacting burners.

Our findings indicate that greater BA and MA flame lengths are associated with higher temperatures in areas opposite the burner, suggesting a long, straight flame. Conversely, a short BA flame length and a long MA flame length correlate with elevated temperatures in adjacent areas, indicating that the flame is bending toward the wall. These localized parameters can be

integrated into combustion control systems to automate adjustments and reduce thermal stress.

Given the interactions among burners, we emphasize the importance of monitoring all burners in a multi-burner setup. This study demonstrates the feasibility of real-time flame measurements in industrial environments, utilizing DL techniques while remaining user-friendly. Future research should investigate strategies to ensure the MA flame length is bending towards the wall and analyze a broader dataset to enhance transferability.

Acknowledgments

Invest BW funds this research for the Ministry of Economics, Labor, and Tourism of Baden-Württemberg, Germany. We want to thank our project partners, the Machine Vision Metrology group at the Institute of Photogrammetry and Remote Sensing at the Karlsruhe Institute of Technology, for the cooperation that enabled the flame segmentation and, in particular, Steven Landgraf for sharing the DL model with us. We are grateful to Laura Kühnlein for her work in the initial project phase, which laid the basis for the thoroughly curated dataset we built on. We want to thank BASF's Hazardous Waste Incineration at the Ludwigshafen site for the opportunity to record data, for providing additional data, and for the dedicated support of their team, especially Stefan Steinle, in carrying out the measurement campaigns. We particularly thank Kai Coenen of BASF for his support and valuable input. Last, we gratefully acknowledge Eva-Maria Klier for her initial research on flame lengths.

References

- Ali, A. M., Tabares, J. D., McGinley, M. W., 2022. A machine learning approach for clinker quality prediction and nonlinear model predictive control design for a rotary cement kiln. *Journal of Advanced Manufacturing and Processing*, 4(4).
- Ballester, J., García-Armingol, T., 2010. Diagnostic techniques for the monitoring and control of practical flames. *Progress in Energy and Combustion Science*, 36(4), 375-411.
- Becker, H., Liang, D., 1978. Visible length of vertical free turbulent diffusion flames. *Combustion and Flame*, 32, 115-137.
- Bunsan, S., Chen, W.-Y., Chen, H.-W., Chuang, Y. H., Grisdanurak, N., 2013. Modeling the dioxin emission of a municipal solid waste incinerator using neural networks. *Chemosphere*, 92(3), 258-264.
- Chu, C., Liu, P., Alsheikh, I., Aydin, F., Serrano-Bayona, R. A., Roberts, W. L., 2024. The flame length measurements of oxygen-enriched carbon dioxide-diluted methane inverse diffusion flames. *Combustion and Flame*, 262, 113282.
- European Commission and Joint Research Centre, Crippa, M., Guizzardi, D., Muntean, M., Schaaf, E., Solazzo, E., Monforti-Ferrario, F., Olivier, J., Vignati, E., 2020. *Fossil CO2 and GHG emissions of all world countries – 2020 report*. Publications Office.
- European Commission and Joint Research Centre, Cusano, G., Roudier, S., Neuwahl, F., Holbrook, S., Gómez Benavides, J., 2019. *Best Available Techniques (BAT) reference document for waste incineration – Industrial Emissions Directive 2010/75/EU (Integrated Pollution Prevention and Control)*. Publications Office.

- Großkopf, J., Matthes, J., Vogelbacher, M., Waibel, P., 2021. Evaluation of Deep Learning-Based Segmentation Methods for Industrial Burner Flames. *Energies*, 14(6).
- Hammerschmid, M., Aguiari, C., Kirnbauer, F., Zerobin, E., Brenner, M., Eisl, R., Nemeth, J., Buchberger, D., Ogris, G., Kolroser, R., Goia, A., Beyweiss, R., Kalch, K., Müller, S., Hofbauer, H., 2023. Thermal Twin 4.0: Digital Support Tool for Optimizing Hazardous Waste Rotary Kiln Incineration Plants. *Waste and Biomass Valorization*, 14(8), 2745-2766.
- Hernández, R., Ballester, J., 2008. Flame imaging as a diagnostic tool for industrial combustion. *Combustion and Flame*, 155(3), 509-528.
- Jiang, Y., Yin, S., Dong, J., Kaynak, O., 2021. A Review on Soft Sensors for Monitoring, Control, and Optimization of Industrial Processes. *IEEE Sensors Journal*, 21(11), 12868-12881.
- Kadlec, P., Gabrys, B., Strandt, S., 2009. Data-driven Soft Sensors in the process industry. *Computers & Chemical Engineering*, 33(4), 795-814.
- Klier, E.-M., 2023. Data-driven characterisation of industrial combustion emissions based on heterogeneous sensor data: carbon monoxide estimation in a hazardous waste incineration plant. Master's thesis, Karlsruhe Institute of Technology.
- Koch, E. W., Rosolowsky, E. W., 2015. Filament identification through mathematical morphology. *Monthly Notices of the Royal Astronomical Society*, 452(4), 3435–3450.
- Landgraf, S., Hillemann, M., Aberle, M., Jung, V., Ulrich, M., 2023a. Segmentation of industrial burner flames: a comparative study from traditional image processing to machine and deep learning. *ISPRS Annals of the Photogrammetry, Remote Sensing and Spatial Information Sciences*, X-1/W1-2023, 953–960.
- Landgraf, S., Hillemann, M., Ulrich, M., Aberle, M., Jung, V., 2023b. Dataset for the segmentation of industrial burner flames.
- Lee, C. W., Kim, I. S., Hong, J. G., 2021. Experimental Investigation on the Effects of the Geometry of the Pilot Burner on Main Flame. *Energies*, 14(4).
- Lu, G., Gilabert, G., Yan, Y., 2005. Vision based monitoring and characterisation of combustion flames. *Journal of Physics: Conference Series*, 15(1), 194.
- Lu, G., Yan, Y., Huang, Y., Reed, A., 1999. An Intelligent Vision System for Monitoring and Control of Combustion Flames. *Measurement and Control*, 32(6), 164-168.
- Matthes, J., Waibel, P., Kollmer, M., Aleksandrov, K., Gehrman, H.-J., Stapf, D., Vogelbacher, M., 2023. Camera based flame stability monitoring and control of multi-burner systems using deep learning based flame detection. *Thermal Science and Engineering Progress*, 41, 101859.
- Norhayati, I., Rashid, M., 2018. Adaptive neuro-fuzzy prediction of carbon monoxide emission from a clinical waste incineration plant. *Neural Computing and Applications*, 30(10), 3049-3061.
- Pani, A. K., Vadlamudi, V. K., Mohanta, H. K., 2013. Development and comparison of neural network based soft sensors for online estimation of cement clinker quality. *ISA Transactions*, 52(1), 19-29.
- ProcessNet Expert Group "Waste Treatment and Recycling", 2022. Position paper "Waste Incineration in the Future".
- Shang, C., You, F., 2019. Data Analytics and Machine Learning for Smart Process Manufacturing: Recent Advances and Perspectives in the Big Data Era. *Engineering*, 5(6), 1010-1016.
- Tang, J., Tian, H., Wang, T., 2024. A Review of Model Predictive Control for the Municipal Solid Waste Incineration Process. *Sustainability*, 16(17).
- van der Walt, S., Schönberger, J. L., Nunez-Iglesias, J., Boulogne, F., Warner, J. D., Yager, N., Gouillart, E., Yu, T., contributors, t. s.-i., 2014. scikit-image: image processing in Python. *PeerJ*, 2.
- Waibel, P., 2014. Konzeption von Verfahren zur kamerabasierenden Analyse und Optimierung von Drehrohrofenprozessen. PhD thesis.
- Xia, H., Tang, J., Yu, W., Qiao, J., 2024. Online Measurement of Dioxin Emission in Solid Waste Incineration Using Fuzzy Broad Learning. *IEEE Transactions on Industrial Informatics*, 20(1), 358-368.
- Yan, Y., Lu, G., Colechin, M., 2002. Monitoring and characterisation of pulverised coal flames using digital imaging techniques. *Fuel*, 81(5), 647-655.
- Yang, Y., Reuter, M. A., Voncken, J. H. L., Verwoerd, J., 2002. Understanding of hazardous waste incineration through computational fluid-dynamics simulation. *J. Environ. Sci. Health*, 37(4), 693–705.
- Zhang, T. Y., Suen, C. Y., 1984. A fast parallel algorithm for thinning digital patterns. *Communications of the ACM*, 27(3), 236–239.
- Zipser, S., Gommlich, A., Matthes, J., Keller, H. B., 2006. Combustion plant monitoring and control using infrared and video cameras. *IFAC Symposium on Power Plants and Power Systems Control*.